Supporting Information

A Combined Computational and Experimental Investigation on the Nature of Hydrated Iodoplumbate Complexes: Insights into the Dual Role of Water in Perovskite Precursor Solutions

Eros Radicchi,[1,2] Francesco Ambrosio,[2,3,*] Edoardo Mosconi,[2] Ahmed A. Alasmari,[4,5] Fatmah A. S. Alasmary,[6] Filippo De Angelis[1,2,3,6 *]

[1]*Department of Chemistry, Biology and Biotechnology, University of Perugia, via Elce di Sotto 8, 06123 Perugia, Italy.*

[2]*Computational Laboratory for Hybrid/Organic Photovoltaics (CLHYO), Istituto CNR di Scienze e Tecnologie Chimiche "Giulio Natta" (CNR-SCITEC), via Elce di Sotto 8, 06123 Perugia, Italy.*

[3]*CompuNet, Istituto Italiano di Tecnologia, Via Morego 30, 16163 Genova, Italy.*

[4] *The First Industrial Institute, TVTC, Riyadh 12613, Saudi Arabia.*

[5]*Physics and Astronomy Department, College of Science, King Saud University, Riyadh 12372, Saudi Arabia.*

[6] *Chemistry Department, College of Science, King Saud University, Riyadh 12372, Saudi Arabia.*

e-mail: francesco.ambrosio@iit,it ; filippo@thch.unipg.it

S1. Equilibrium dissociation constants of aqueous iodoplumbates from a grand-canonical formulation of solutes in aqueous solution

To calculate the equilibrium dissociation constants of iodoplumbates in aqueous solution, we employ a grand-canonical formulation of solutes in aqueous solution.[1] Considering the generic dissociation reaction:

$$\mathrm{PbI_x^z(aq) \rightleftarrows PbI_{x-1}^{z+1}(aq) + I^-(aq)} \tag{S1}$$

we can define K_d^x as:

$$K_{\mathrm{d}}^{\mathrm{x}} = \frac{[\mathrm{PbI_{x-1}^{z+1}(aq)}][\mathrm{I^-(aq)}]}{[\mathrm{PbI_x^z(aq)}]}. \tag{S2}$$

The concentration of a solute X with a charge state q in solution can be expressed from the respective formation energy, $\mathrm{G_f}[X(aq)]$, Eq. (S3): [1, 2]

$$\mathrm{c_X(aq)} = c_0 e^{-G_f^q[\mathrm{X(aq)}]/k_B T}, \tag{S3}$$

where c_0 is the number of water moles in 1 L of liquid water (55.5 mol/L), T is the temperature (in K), and k_B is the Boltzmann constant. From Eqs. (S2) and (S3), we obtain:

$$K_{\mathrm{d}}^{\mathrm{x}} = \frac{c_0 e^{-G_f^q[\mathrm{PbI_{x-1}^{z+1}(aq)}]/k_B T} c_0 e^{-G_f^q[\mathrm{I^-(aq)}]/k_B T}}{c_0 e^{-G_f[PbI_x^z(aq)]/k_B T}}, \tag{S4}$$

$$\mathrm{p}K_{\mathrm{d}}^{\mathrm{x}} = \frac{G_f^q[\mathrm{PbI_{x-1}^{z+1}(aq)}] + G_f[\mathrm{I^-(aq)}] - G_f^q[\mathrm{PbI_x^z(aq)}]}{\ln 10\, k_B T} - \log(c_0). \tag{S5}$$

The formation Gibbs free energy of a solute X in a charge state q is given by Eq. (S6):[1]

$$G_f^q[\mathrm{X(aq)}] = G^q[\mathrm{X(aq)}] - G[\mathrm{bulk}] - \sum_i n_i\mu_i + q(\varepsilon_{v-w} + \mu_e) + E_{corr}^q \quad \text{(S6)}$$

where $G^q[\mathrm{X(aq)}]$ is the Gibbs free energy of the solute X in the charged state q, $G[\mathrm{bulk}]$ the Gibbs free energy of bulk water, μ_i the chemical potential of the added/subtracted species i, n_i the number of added/subtracted i atoms, ε_{v-w} is the valence band edge of bulk liquid water, μ_e the electron chemical potential, and E_{corr}^q a correction term taking into account electrostatic finite-size effects. In this work, the Freysoldt–Neugebauer–Van de Walle scheme[3, 4] is employed to correct the total energies achieved with calculations of periodic charged supercells. We note that for the considered supercells, calculated electrostatic finite-size corrections are below 0.03 eV, due to the high static dielectric constant of liquid water at ambient conditions (78.3).[5] Therefore, we do not include the respective terms in the following.

By applying the formulation of Eq. (S6) into Eq. (S5), we obtain the following expression:

$$pK_d^x = \frac{G[\mathrm{PbI}_{x-1}^{z+1}(\mathrm{aq})] - G[\mathrm{PbI}_x^z(\mathrm{aq})]}{\ln 10\, k_B T} + \frac{+\,G[\mathrm{I}^-(\mathrm{aq})] - G[\mathrm{bulk}]}{\ln 10\, k_B T} - \log(\mathrm{c}_0) \quad \text{(S7)}$$

Free energy differences are here calculated using the thermodynamic integration. In this technique, an auxiliary Hamiltonian is defined as a linear combination of the Hamiltonians of the reactant and the product:[6, 7]

$$H_\eta = (1-\eta)H_R + \eta H_P \quad \text{(S8)}$$

where $0 < \eta < 1$ is the Kirkwood coupling parameter.[6, 7] For each value of η, the time-averaged vertical energy difference between the reactant and the product $< \Delta E >_\eta$ is calculated. The free energy change of the reaction ΔA is given by the integration of the $< \Delta E >_\eta$ values calculated at varying η:

$$\Delta A = A(P) - A(R) = A(\eta = 1) - A(\eta = 0) = \int_0^1 < \Delta E >_\eta d\eta \quad \text{(S9)}$$

In this way, the free energy differences reported in Eq. (S7) can be evaluated, as follows:

$$G[\mathrm{PbI}_{x-1}^{z+1}(\mathrm{aq})] - G[\mathrm{PbI}_x^z(\mathrm{aq})] = \int_0^1 < \Delta_{\mathrm{dI}} E_{\mathrm{PbI}_x^z}(\mathrm{aq}) >_\eta d\eta, \quad \text{(S10)}$$

$$\int_0^1 < \Delta_{\mathrm{dI}} E_{\mathrm{PbI}_x^z}(\mathrm{aq}) >_\eta d\eta = \Delta_{\mathrm{dI}} A_{\mathrm{PbI}_x^z}(\mathrm{aq}) - \Delta_{\mathrm{zp}} E_{\mathrm{PbI}_x^z}(\mathrm{aq}), \quad \text{(S11)}$$

and

$$G[\mathrm{bulk}] - G[\mathrm{I}^-(\mathrm{aq})] = \int_0^1 < \Delta_{\mathrm{dI}} E_{\mathrm{I}^-}(\mathrm{aq}) >_\eta d\eta\,, \quad \text{(S12)}$$

$$\int_0^1 < \Delta_{\mathrm{dI}} E_{\mathrm{I}^-}(\mathrm{aq}) >_\eta d\eta = \Delta_{\mathrm{dI}} A_{\mathrm{I}^-}(\mathrm{aq}) - \Delta_{\mathrm{zp}} E_{\mathrm{I}^-}(\mathrm{aq})\,. \quad \text{(S13)}$$

In Eqs. (S10-S13), $\Delta_{\mathrm{dI}} A_{\mathrm{PbI}_x^z}(\mathrm{aq})$ and $\Delta A_{\mathrm{I}^-}(\mathrm{aq})$ are the thermodynamic integral associated with the removal of an iodide from a $\mathrm{PbI}_x^z(\mathrm{aq})$ iodoplumbate and from $\mathrm{I}^-(\mathrm{aq})$, $\Delta_{\mathrm{zp}} E_{\mathrm{PbI}_x^z}(\mathrm{aq})$ and $\Delta_{\mathrm{zp}} E_{\mathrm{I}^-}(\mathrm{aq})$ are the zero-point motion corrections, which accounts for the error due to the classical treatment of the nuclei in DFT-MD simulations.

Thermodynamic integrals are here calculated by adopting the Marcus approximation since it has been proved to provide accurate results in previous studies.[1, 8, 9] In this method, we consider two values of the Kirkwood coupling parameter η (0 and 1), thus giving:

$$\Delta_{\mathrm{dI}} A_{\mathrm{PbI}_x^z}(\mathrm{aq}) = \frac{<\Delta_{\mathrm{dI}} E_{\mathrm{PbI}_x^z}(\mathrm{aq})>_0 + <\Delta_{\mathrm{dI}} E_{\mathrm{PbI}_x^z}(\mathrm{aq})>_1}{2}, \quad \text{(S14)}$$

$$\Delta_{\mathrm{dI}} A_{\mathrm{I}^-}(\mathrm{aq}) = \frac{<\Delta_{\mathrm{dI}} E_{\mathrm{I}^-}(\mathrm{aq})>_0 + <\Delta_{\mathrm{dI}} E_{\mathrm{I}^-}(\mathrm{aq})>_1}{2}\,. \quad \text{(S15)}$$

Energy differences at $\eta = 0$ are those related with the vertical detachment of an iodide anion from the simulation cell. The average value is calculated from 50 snapshots equally spaced in time from the trajectory achieved for each iodoplumbate: PbI^+, PbI_2, PbI_3^- and PbI_4^{2-}.

The sampling of energy differences at $\eta = 1$ corresponds to the vertical insertion of an iodide anion. In this case, we insert an I^- close to the $PbI_{x-1}^{z+1}(aq)$ iodoplumbate for $< \Delta_{dI} E_{PbI_x^z}(aq) >_1$ (in a void in liquid water for $< \Delta_{dI} E_{I^-}(aq) >_1$). Then, we perform a structural relaxation in which all atoms except the inserted I^- are fixed. This is done for 15-30 snapshots.

The zero-point motion correction $\Delta_{zp} E_{PbI_x^z}(aq)$ is calculated as the difference in zero-point energies between $PbI_x^z(aq)$ and $PbI_{x-1}^{z+1}(aq)$, which correspond to the zero-point energy associated with iodide in the $PbI_x^z(aq)$ complexes. Therefore, for each case, we calculate the three vibrational frequencies of the related normal modes and the zero-point energy as:

$$\Delta_{zp} E = \sum_{n=1}^{3} \frac{h\upsilon_i}{2} \tag{S16}$$

where h is the Planck constant and υ_i the frequency of the *i*-th normal mode. For all the studied complexes, the correction terms are negligible (< 30 meV) due to the low frequencies of the associated vibrational modes (< 140 cm^{-1}). Likewise, $\Delta_{zp} E_{I^-}(aq)$, calculated from the vibrational frequencies of the $I^-(aq)$ complex, is negligible.

Therefore, we evaluate the dissociation constants from this final simplified expression:

$$pK_d^x = \frac{\Delta_{dI} A_{PbI_x^z}(aq) - \Delta_{dI} A_{I^-}(aq)}{\ln 10 \; k_B T} - \log(c_0) \tag{S17}$$

From Table S1, we observe that larger iodoplumbates show a stronger tendency to dissociate, in agreement with the trend experimentally observed. The quantitative agreement with the experiment is,

however, limited to ~4 pK units, corresponding to ~0.2 eV, which is the estimated accuracy of the method.[1, 10]

Table S1. Calculated values of $\Delta\Delta_{\mathrm{dI}}\mathrm{A} = \Delta_{\mathrm{dI}}\mathrm{A}_{\mathrm{PbI}_x^z}(\mathrm{aq}) - \Delta_{\mathrm{dI}}\mathrm{A}_{\mathrm{I}^-}(\mathrm{aq})$ (eV) and pK_d^x, along with the experimental range of values inferred from Refs. 11, 12.

Reaction	$\Delta\Delta_{\mathrm{dI}}\mathrm{A}$	pK_d^x(theory)	pK_d^x (expt.[11, 12])
$PbI^+ \rightarrow Pb^{2+} + I^-$	0.29 eV	3.2	1.3-2.00
$PbI_2 \rightarrow PbI^+ + I^-$	0.15 eV	0.8	1.2-1.5
$PbI_3^- \rightarrow PbI_2 + I^-$	−0.12 eV	−3.7	0.6-0.8
$PbI_4^{2-} \rightarrow PbI_3^- + I^-$	−0.11 eV	−3.6	0.5-1.50

S2. Structural analysis of aqueous iodoplumbates

Solvated PbI^+ shows an average Pb−I distance of 3.14 Å, Figure S1, with a secondary distribution centered at 3.55 Å representing a minority of structural configurations in which iodide is less bonded to the metal cation. Solvated PbI_2 has a *cis* arrangement of the PbI_2 moiety geometry with an average I-Pb-I angle of 95.5º, Figure 1b in the main text. The distribution of Pb−I distances is broadened and the small peak encountered for aqueous PbI^+ sharpens, a clear hint to the weakening of the Pb−I interaction as the number of coordinating I^- is increased, Figure S1. The trend observed in the solvation of Pb^{2+}, PbI^+, and PbI_2 can be extended to aqueous PbI_3^- and PbI_4^{2-}. The first solvation shell is more rigid and cannot accommodate a large number of water molecules. As a consequence, the global coordination of Pb^{2+} is reduced to six-fold with n_O equal to 2.93 (86%) and 1.93 (91%), for PbI_3^- and PbI_4^{2-}, respectively. Consistently, the first peak of the Pb−O RDF is shifted towards a higher distance, ~2.75 Å. In both cases, Pb^{2+} is found to be coordinated in a distorted octahedral geometry, Figure 1b in the main text. PbI_3^- features three iodide ions on the same molecule side thus representing a case of hemidirected coordination. Similar considerations apply for aqueous PbI_4^{2-}. The distribution of Pb−I distances for both complexes features an enhanced tail at long distances, particularly for PbI_4^{2-}, thus suggesting a further decrease in the strength of the interactions between the lead cation and the coordinating iodide anions, Figure S1.

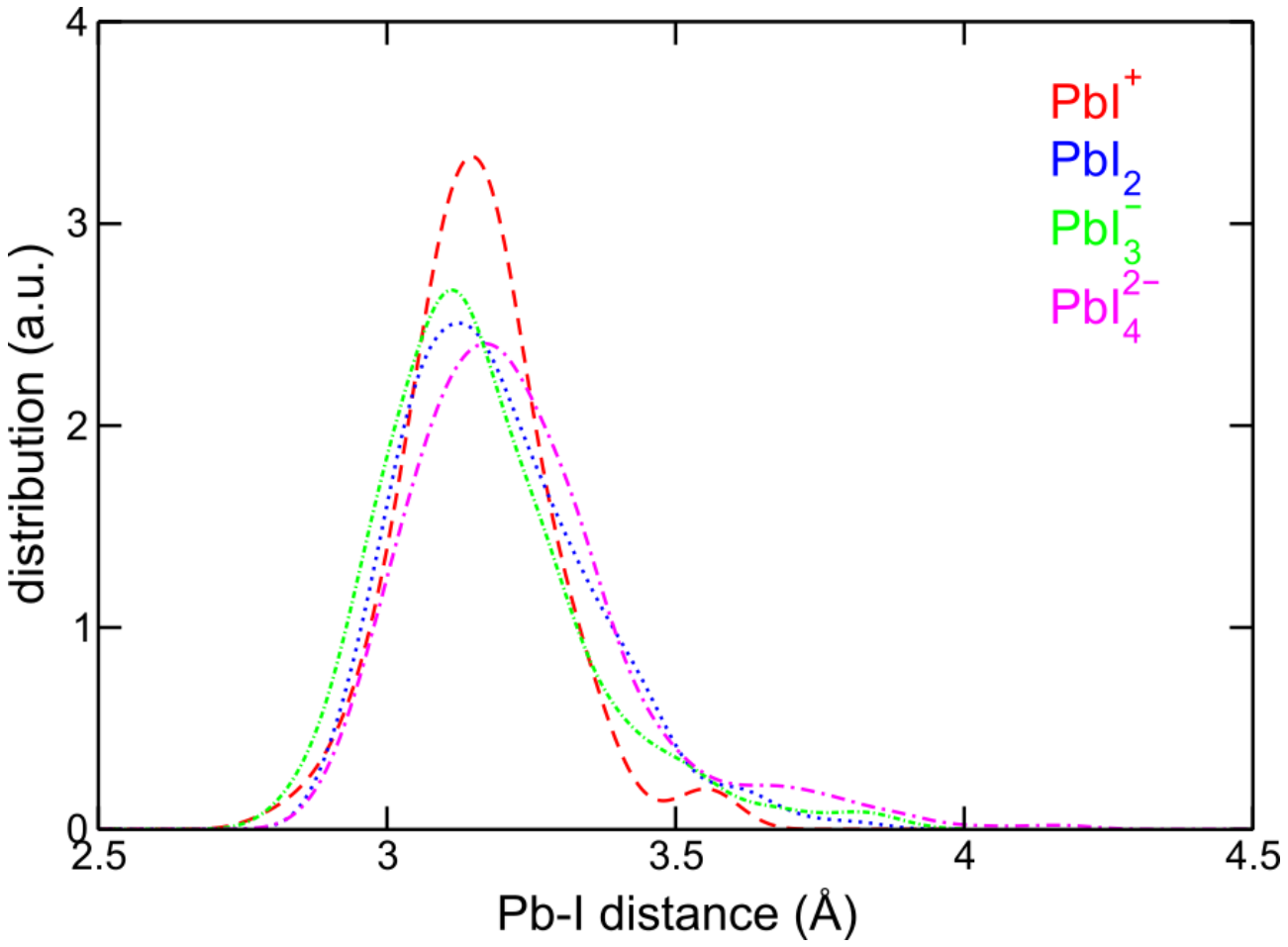

Figure S1. Distribution of Pb-I distances for aqueous PbI^+ (red), PbI_2 (blue), PbI_3^- (green), and PbI_4^{2-} (magenta).

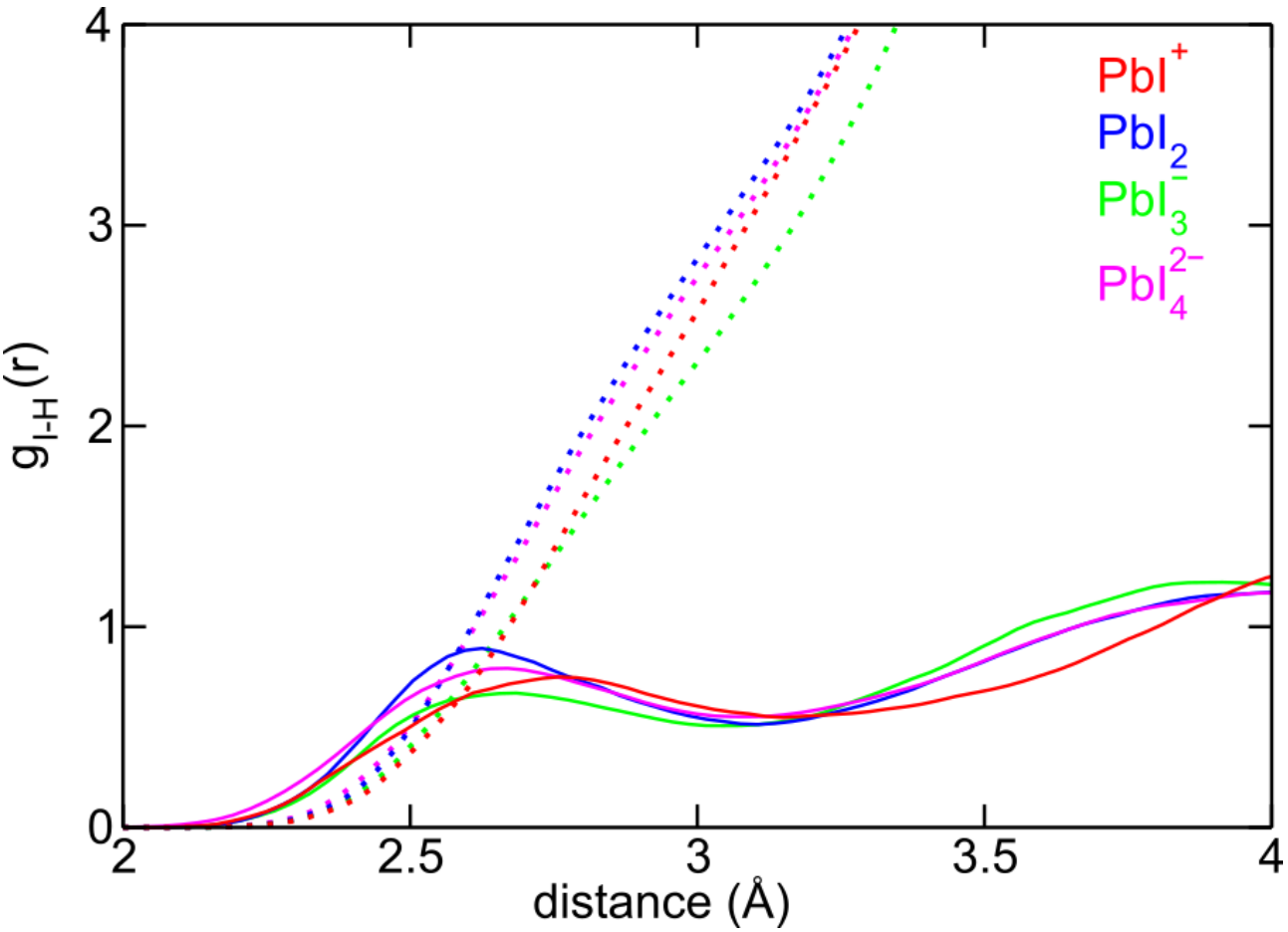

Figure S2. I−H radial distribution functions (RDFs) for aqueous PbI^+ (red), PbI_2 (blue), PbI_3^- (green) and PbI_4^{2-} (magenta). Dashed lines for the respective normalized integral.

S3. Concentration of species in PbI_2 solutions evaluated with the Spana software

Table S2. Estimated concentrations of the species present in a PbI_2 solution, varying its concentration (from 2.00×10^{-3} to 6.04×10^{-1} mM).

PbI_2 solution concentration (mM)	$[Pb^{2+}]$ (mM)	$[PbI^{+}]$ (mM)	$[PbI_2]$ (mM)	$[PbI_3^{-}]$ (mM)	$[I^{-}]$ (mM)
2.00×10^{-3}	2.00×10^{-3}	0	0	0	3.98×10^{-3}
4.00×10^{-3}	3.98×10^{-3}	3.24×10^{-6}	0	0	7.94×10^{-3}
8.00×10^{-3}	7.94×10^{-3}	1.32×10^{-5}	0	0	1.62×10^{-2}
1.21×10^{-2}	1.17×10^{-2}	2.88×10^{-5}	0	0	2.51×10^{-2}
1.61×10^{-2}	1.55×10^{-2}	5.13×10^{-5}	0	0	3.24×10^{-2}
2.01×10^{-2}	2.00×10^{-2}	7.94×10^{-5}	0	0	3.98×10^{-2}
4.03×10^{-2}	3.98×10^{-2}	3.31×10^{-4}	0	0	7.94×10^{-2}
6.04×10^{-2}	5.89×10^{-2}	7.08×10^{-4}	0	0	1.20×10^{-1}
8.05×10^{-2}	7.94×10^{-2}	1.23×10^{-3}	3.24×10^{-6}	0	1.62×10^{-1}
1.01×10^{-1}	9.77×10^{-2}	1.95×10^{-3}	6.17×10^{-6}	0	1.95×10^{-1}
1.51×10^{-1}	1.51×10^{-1}	4.47×10^{-3}	2.09×10^{-5}	0	2.88×10^{-1}
2.01×10^{-1}	2.00×10^{-1}	7.59×10^{-3}	4.79×10^{-5}	0	3.98×10^{-1}
2.52×10^{-1}	2.45×10^{-1}	1.17×10^{-2}	9.12×10^{-5}	0	4.90×10^{-1}

3.02×10^{-1}	2.95×10^{-1}	1.66×10^{-2}	1.58×10^{-4}	0	5.89×10^{-1}
4.03×10^{-1}	3.72×10^{-1}	2.95×10^{-2}	3.47×10^{-4}	1.41×10^{-6}	7.59×10^{-1}
5.03×10^{-1}	4.57×10^{-1}	4.27×10^{-2}	6.61×10^{-4}	3.16×10^{-6}	9.77×10^{-1}
6.04×10^{-1}	5.25×10^{-1}	6.31×10^{-2}	1.12×10^{-3}	6.46×10^{-6}	1.12

The concentration of species in a PbI_2 solution are evaluated assuming that all the PbI_2 is solvated, thus assuming that, in the concentration range here considered, the precipitation equilibrium of PbI_2 can be neglected. Concentrations of aqueous PbI_4^{2-} are negligible and not reported in Table S2.

S4. Extended spectra of aqueous iodoplumbates

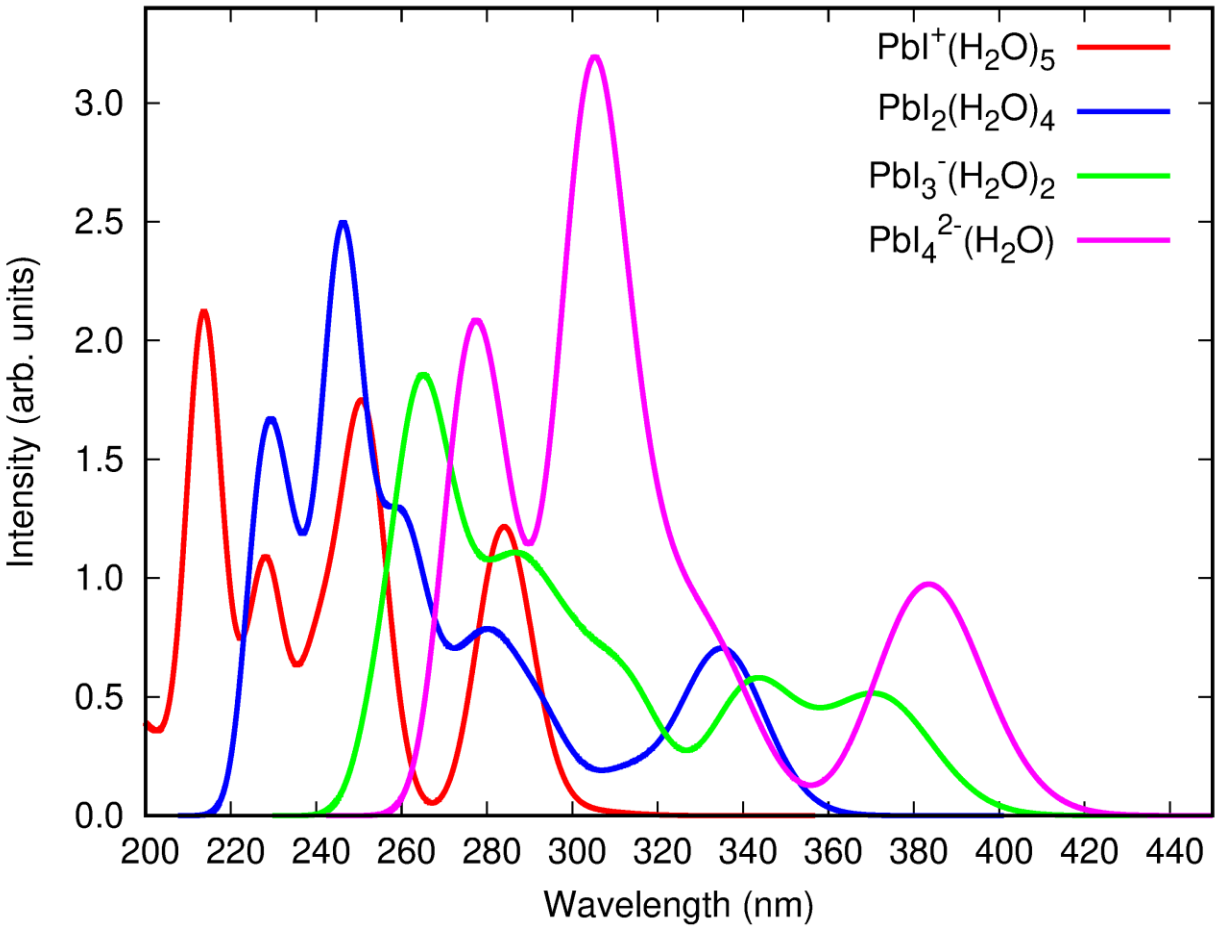

Figure S3. Extended theoretical spectra (60 lowest energy excited states) of optimized complexes of PbI^+ and PbI_2 with a total coordination number of 6 and PbI_3^- and PbI_4^{2-} with a total coordination number of 5.

S5. Absorption spectra vs number of water molecules

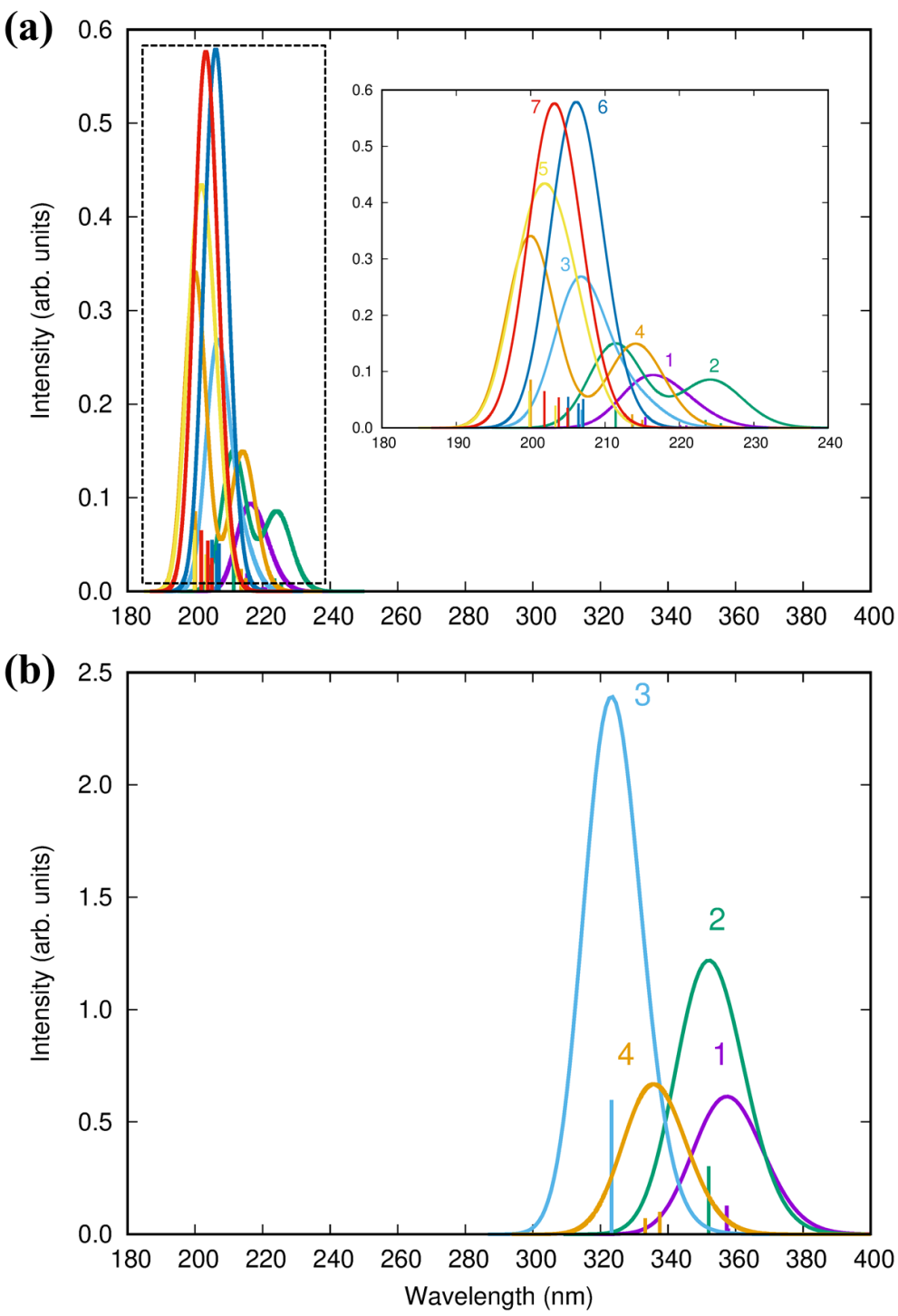

Figure S4. Theoretical absorption spectra of aqueous (a) Pb^{2+} (inset: zoom on the 180-240 nm region) and (b) PbI_2 at different number of explicit water molecules included in the calculation.

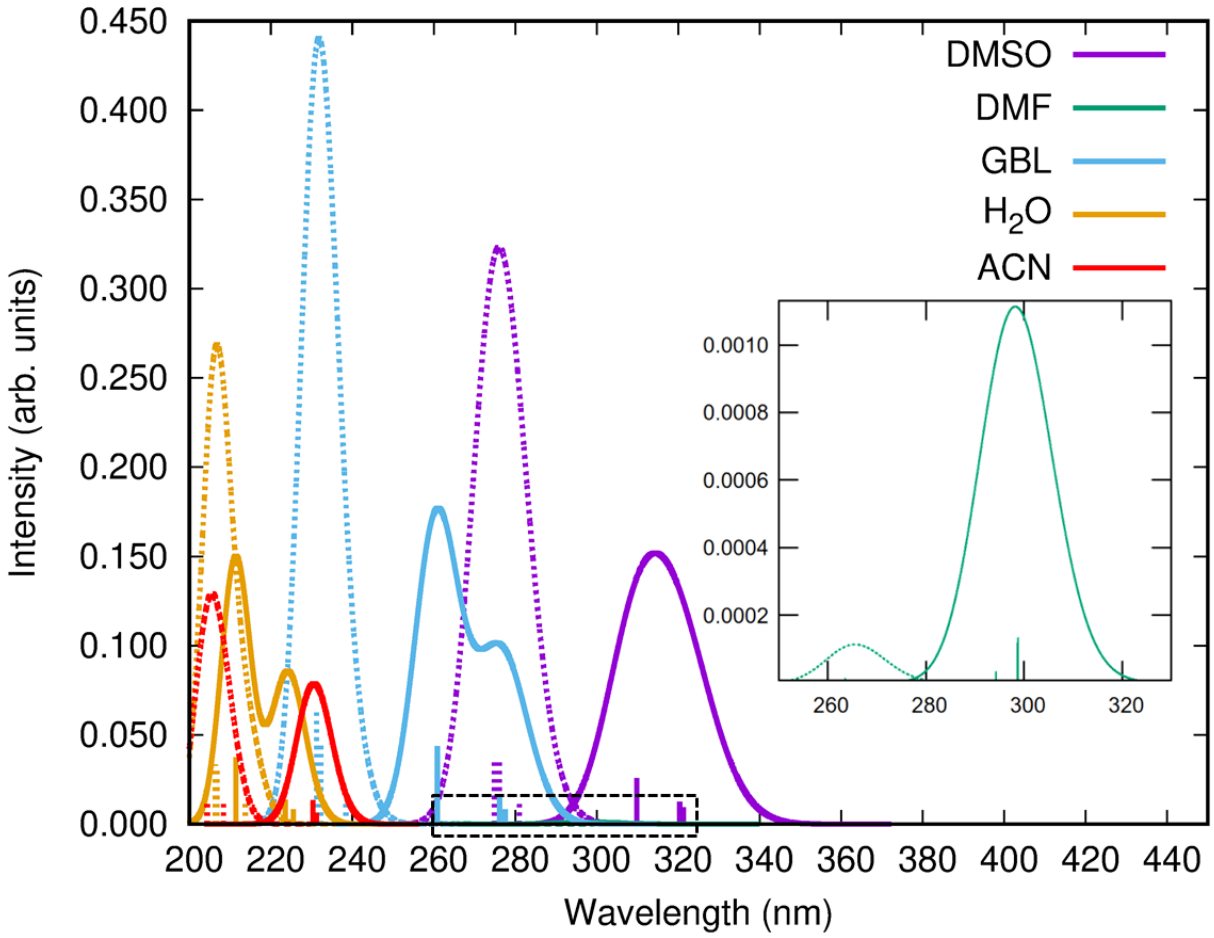

Figure S5. Theoretical absorption spectra of $Pb^{2+}(solv)_2$, continuous lines, and $Pb^{2+}(solv)_3$, dotted lines, for solv = DMSO, DMF, GBL, ACN and H_2O. In the inset, we report the magnification of the DMF spectra, that show low absorption intensity.

S6. Structural analysis of aqueous iodide

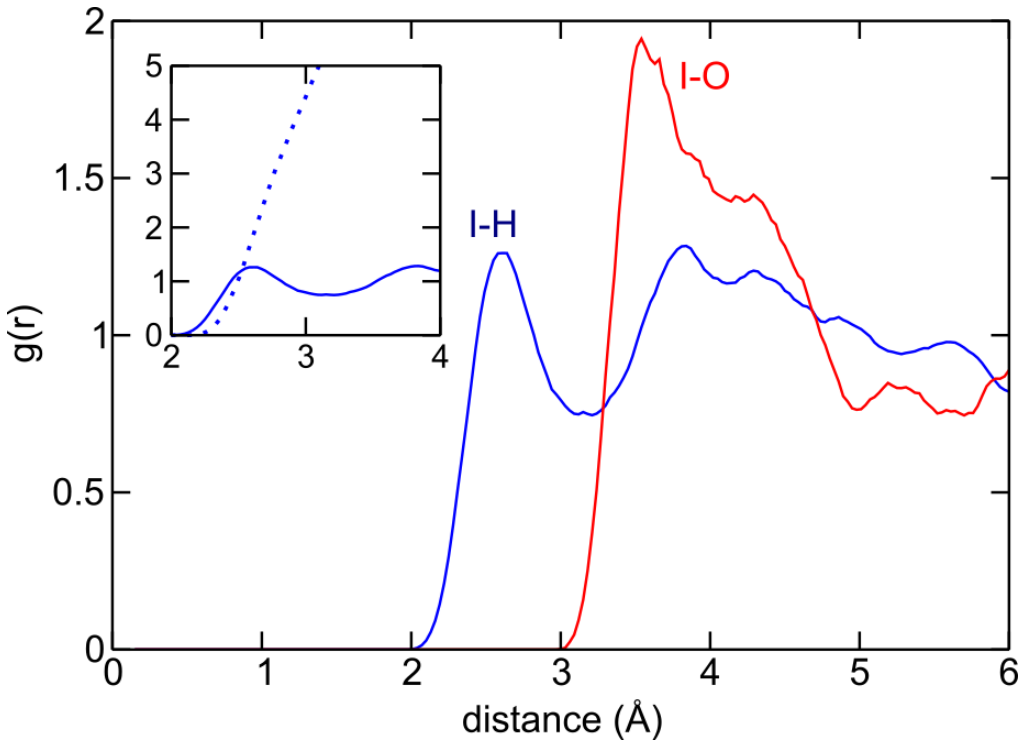

Figure S6. I-H (blue) and I-O (red) radial distribution functions (RDFs) for aqueous I^-. In the inset, we report the I-H radial distribution function along with the normalized integral.

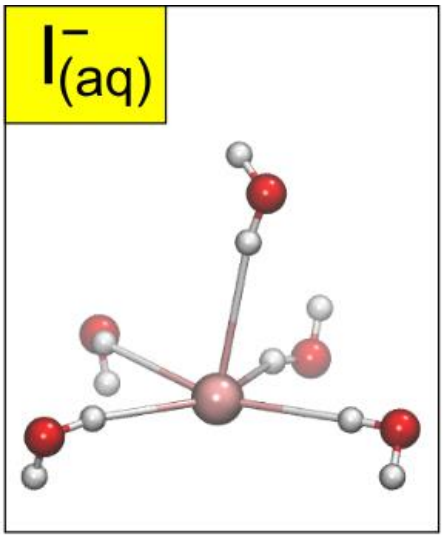

Figure S7. Stick&ball representation of a configuration of aqueous iodide as achieved from molecular dynamics simulation. O atoms in red, H in white, and I in pink.

Iodide in aqueous solution coordinates on average 4.8 water molecules, as inferred from the integration of the first peak of the I-O radial distribution reported in Figure S6, with hydrogen atoms of surrounding water molecules pointing towards the anion, Figure S7. The I-H (I-O) radial distribution function peaks at 2.58 (3.54) Å, in line with previous simulations.[13]

References

1. Ambrosio, F.; Miceli, G.; Pasquarello, A., Redox Levels in Aqueous Solution: Effect of van der Waals Interactions and Hybrid Functionals. *J. Chem. Phys.* **2015,** *143* (24), 244508.

2. Todorova, M.; Neugebauer, J., Extending the Concept of Defect Chemistry from Semiconductor Physics to Electrochemistry. *Phys. Rev. Appl.* **2014,** *1* (1), 014001.

3. Freysoldt, C.; Neugebauer, J.; Van de Walle, C. G., Fully Ab Initio Finite-Size Corrections for Charged-Defect Supercell Calculations. *Phys. Rev. Lett.* **2009,** *102* (1), 016402.

4. Komsa, H.-P.; Rantala, T. T.; Pasquarello, A., Finite-Size Supercell Correction Schemes for Charged Defect Calculations. *Phys. Rev. B* **2012,** *86* (4), 045112.

5. Malmberg, C. G. M., Maryott; A. A., Dielectric Constant of Water from 0 to 100 C. *Journal of Research of the National Bureau of Standards* **1956,** *56* (1).

6. Frenkel, D.; Smit, B., Chapter 8 - The Gibbs Ensemble. In *Understanding Molecular Simulation (Second Edition)*, Frenkel, D.; Smit, B., Eds. Academic Press: San Diego, 2002; pp 201-224.

7. Kirkwood, J. G., Statistical Mechanics of Fluid Mixtures. *J. Chem. Phys.* **1935,** *3* (5), 300-313.

8. Ambrosio, F.; Wiktor, J.; Pasquarello, A., pH-Dependent Surface Chemistry from First Principles: Application to the BiVO4(010)–Water Interface. *ACS Appl. Mater. Interfaces* **2018,** *10* (12), 10011-10021.

9. Ambrosio, F.; Miceli, G.; Pasquarello, A., Structural, Dynamical, and Electronic Properties of Liquid Water: A Hybrid Functional Study. *J. Phys. Chem. B* **2016,** *120* (30), 7456-7470.

10. Cheng, J.; Sprik, M., Alignment of Electronic Energy Levels at Electrochemical Interfaces. *Phys. Chem. Chem. Phys.* **2012,** *14* (32), 11245-11267.

11. Clever, H. L.; Johnston, F. J., The Solubility of Some Sparingly Soluble Lead Salts: An Evaluation of the Solubility in Water and Aqueous Electrolyte Solution. *J. Phys. Chem. Ref. Data* **1980,** *9* (3), 751-784.

12. Tur'yan, Y. I., *Zh. Neorg. Khim.* **1961,** *6*, 162-164.

13. Heuft, J. M.; Meijer, E. J., Density Functional Theory Based Molecular-Dynamics Study of Aqueous Iodide Solvation. *J. Chem. Phys.* **2005,** *123* (9), 094506.